JOURNAL OF SOLID STATE CHEMISTRY 40, 352–360 (1981)

An Order–Disorder Transition in Sr_2IrD_5: Evidence for Square Pyramidal IrD_5 Units from Powder Neutron Diffraction Data

JIAN ZHUANG,* JULIUS M. HASTINGS,† AND LESTER M. CORLISS†‡

Department of Chemistry, Brookhaven National Laboratory, Upton, New York 11973

AND R. BAU AND CHIAU-YU WEI

Department of Chemistry, University of Southern California, University Park, Los Angeles, California 90007

AND R. O. MOYER, JR.

Department of Chemistry, Trinity College, Hartford, Connecticut 06106

Received August 28, 1981

Neutron diffraction data have been collected on a powdered sample of Sr_2IrD_5 over a range of temperatures. The compound, which is cubic at room temperature, has been found to exhibit a gradual transformation to a tetragonal phase in the temperature range 200–140 K. As a result of the transition, deuterium atoms which randomly occupy sixfold positions in the cubic phase, become tetragonally ordered. A small fraction of the cubic phase remained untransformed at 4.2 K. Both the cubic and tetragonal structures are consistent with square pyramidal IrD_5 units with average Ir–D distances of 1.714 and 1.718 Å, respectively. Agreement factors, R_1, for the two structural analyses are 3.44 and 4.94%.

Introduction

The room temperature crystal structure of the ternary deuteride Sr_2IrD_5 has been determined previously, using X-ray and neutron diffraction, by Moyer *et al.* (*1*). Their results, indicating random occupancy of the sixfold deuterium sites, are confirmed in the present work. We report, in addition, that at low temperatures, most of the compound undergoes a cubic-to-tetragonal phase transformation, accompanied by a slight lattice distortion and an ordering of deuterium atoms. In the following we describe neutron diffraction studies of the high- and low-temperature phases, and of the evolution of the phase transformation.

* Permanent address: Fujian Institute of Research on the Structure of Matter, Fuzhou, Fujian, China.

† Research carried out at Brookhaven National Laboratory under contract with the U.S. Department of Energy and supported by its Office of Basic Energy Sciences.

‡ Author to whom correspondence should be addressed.

Experimental

Sample Preparation

Strontium rod, purchased from A. D.

0022-4596/81/150352-09$02.00/0

Mackay, Inc., was purified by vacuum distillation at 800°C. Iridium powder (−325 mesh and 99.9% pure) was purchased from Alfa Division of Ventron Corp. Chemically pure grade (99.5 at.% minimum) deuterium was purchased from Matheson Gas Products, and prepurified argon (99.998 at.% minimum) was obtained from Airco Industrial Gases.

Strontium iridium deuteride was prepared in two steps. First, SrD_2 was formed by heating chips of the vacuum-distilled strontium metal in deuterium at 460°C. The SrD_2 was easily crushed into a very fine powder using an agate mechanical ball mill. Strontium deuteride powder was combined with the iridium powder in a 2: 1 mole ratio and mixed by tumbling for approximately 10 min. The homogeneous powder was compressed at 5000 psi into a 0.25-in.-diameter cylindrical pellet. The pellet was placed into a molybdenum boat which was then inserted into a quartz sleeve. The sleeve was loaded into a quartz reaction tube, and the tube was attached to a glass vacuum line. The system was evacuated to 1×10^{-5} Torr after which deuterium was admitted to approximately 700 Torr. The pellet was heated at 760°C for approximately 18 hr. The product was cooled quickly by withdrawing the furnace from the reaction tube, and subsequently crushed into a fine powder with a mechanical agate mill. Metals and deuterides were handled in a glovebag under a protective argon atmosphere.

X-Ray diffraction data for Sr_2IrD_5 were consistent with the data reported for Sr_2IrH_5 (*1*), and the X-ray diffractometer tracing for a sample of Sr_2IrD_5 indicated the presence of the ternary deuteride phase only.

Approximately 6 g of Sr_2IrD_5 were transferred into a quartz ampoule (15 mm o.d.,

TABLE I

CRYSTALLOGRAPHIC DATA FOR CUBIC Sr_2IrD_5 AT ROOM TEMPERATURE (SPACE GROUP $Fm3m$)

	Results of present work	Results reported by Moyer *et al.* (*1*)
Cell constant a (Å)	7.6464 (±0.0009)	7.62
Atomic positions	Sr: $8c(\frac{1}{4}, \frac{1}{4}, \frac{1}{4})$ Ir: $4a(0, 0, 0)$ D: $24e(x, 0, 0)$ with x = 0.2242 ± 0.0007	Sr: $8c(\frac{1}{4}, \frac{1}{4}, \frac{1}{4})$ Ir: $4a(0, 0, 0)$ D: $24e(x, 0, 0)$ with x = 0.233 ± 0.002
Occupation number of D sites η_D	0.87 (±0.02)	0.83 (±0.05)
Atomic ratio (D/Sr_2 or D/I_r)	5.2 (±0.1)	5.0 (±0.3)
Isotropic thermal parameters		
B_{Sr}	0.6 (±0.2)	0.3 (±0.3)
B_{Ir}	0.8 (±0.1)	1.8 (±0.3)
B_D	2.2 (±0.2)	1.6 (±0.2)
R factors (*2*)		
R_1	3.44	9
R_2	14.66	—

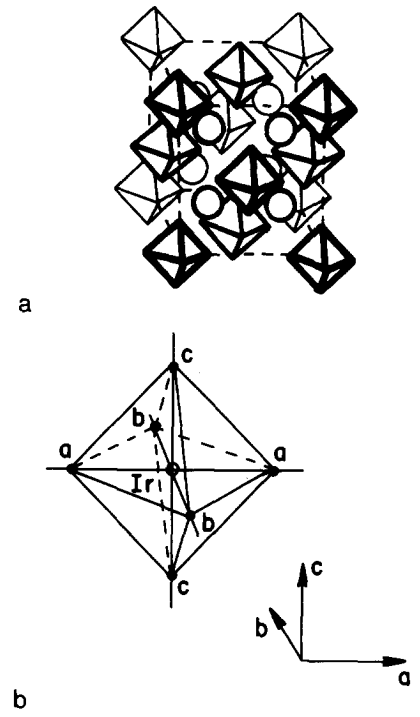

FIG. 1. Crystal structure of Sr_2IrD_5 at room temperature. In (a) the Sr^{+2} ions are represented by circles and the $[IrD_5]^{4-}$ ions by octahedra. The randomly occupied deuterium sites are labeled in (b) to correspond with the crystallographic axes.

12 mm i.d., and 90 mm long). The ampoule was then evacuated and sealed for temporary storage.

Data Collection and Analysis

The neutron powder data were obtained with a three-crystal spectrometer, using a Ge(111) monochromator and a pyrolytic graphite (004) analyzer. Horizontal collimation was provided by Soller slits with 20′ divergence before and after the monochromator, as well as after the sample, and 40′ between the analyzer and counter. This instrumental configuration greatly extended the angular range of usable diffraction data without unacceptable sacrifice of intensity. The sample was contained in a helium-filled cylindrical cell mounted in a variable-temperature cryostat capable of reaching 4.2 K. In the intermediate temperature range, temperatures were controlled to 0.1 K.

Diffraction data in the range $13° < 2\theta < 120°$ were collected using a neutron wavelength of 1.3102 Å and 2θ scanning steps of 0.1°. A profile-fitting least-squares refinement program, originally written by Rietveld (*2*) and subsequently modified by Hewat (*3*), was used in interpreting the diagrams. Isotropic temperature factors were employed and the occupation numbers of the deuterium sites were refined without

TABLE II

OBSERVED AND CALCULATED NEUTRON DIFFRACTION DATA FOR CUBIC Sr_2IrD_5 AT ROOM TEMPERATURE

$h\ k\ l$	2θ (°)	I_{obs}	I_{calc}
1 1 1	17.04	2006	1992
2 0 0	19.72	282	324
2 2 0	28.02	884	909
2 2 2	34.50	2223	2141
4 0 0	40.06	3066	3027
3 3 1	43.83	26	25
4 2 0	45.03	96	95
4 2 2	49.61	527	508
5 1 1	52.84	1097	1053
3 3 3	52.84	8	8
4 4 0	57.95	2433	2456
5 3 1	60.88	882	776
6 0 0	61.84	41	43
4 4 2	61.84	11	12
4 4 4	72.80	902	905
7 1 1	75.42	41	40
5 5 1	75.42	748	727
6 4 0	76.29	64	56
7 3 1	82.28	2	2
5 5 3	82.28	378	366
8 0 0	86.51	437	448
7 3 3	89.03	12	11
8 2 2	93.24	126	147
6 6 0	93.24	219	254
7 5 1	95.77	202	186
5 5 5	95.77	215	198
6 6 2	96.62	320	297
8 4 0	100.02	1325	1266
9 1 1	102.59	283	305
7 5 3	102.59	54	59

constraints. Tabulated R factors are defined in Ref. (*2*).

The Structure of Sr_2IrD_5 at Room Temperature

The structure of Sr_2IrD_5 at room temperature, as reported by Moyer, *et al.*, may be described as follows:

Composition: $Sr_2IrD_{5.0\pm0.3}$;
Space group: $Fm3m$ (No. 225), four formula units per cell; a = 7.62 Å;
Atomic positions: Sr in 8*c*; Ir in 4*a*, D in 24*e* with x = 0.233.

The structure can be visualized as shown in Fig. 1a. There the circles represent the strontium sites; the centers of the octahedra are occupied by iridium; and the six vertices of each octahedron are randomly occupied by 5.0 ± 0.3 deuterium atoms. The six deuterium sites surrounding each iridium atom can be divided into three subsets denoted as D_a, D_b, D_c in Fig. 1b. Based upon this model, a least-squares refinement was carried out to fit our observed data. Table I gives the results of the refinement. The values reported previously by Moyer *et al.* (*1*) are added for comparison.

Attempts to refine in other space groups gave no significant improvement despite the introduction of additional parameters. Calculated intensities are presented in Table II, where they are seen to be in quite good agreement with the observed values. Those reflections that are overlapped by aluminum lines from the sample holder have been omitted. The calculated profile is given in Fig. 2a. Inspection of Fig. 2a shows two weak diffraction peaks at 29.4 and 42.0° that do not index on the Sr_2IrD_5 cell. They are almost certainly due to the presence of a small amount of SrO in the sample. According to Swanson *et al.* (*4*), these angular positions correspond exactly

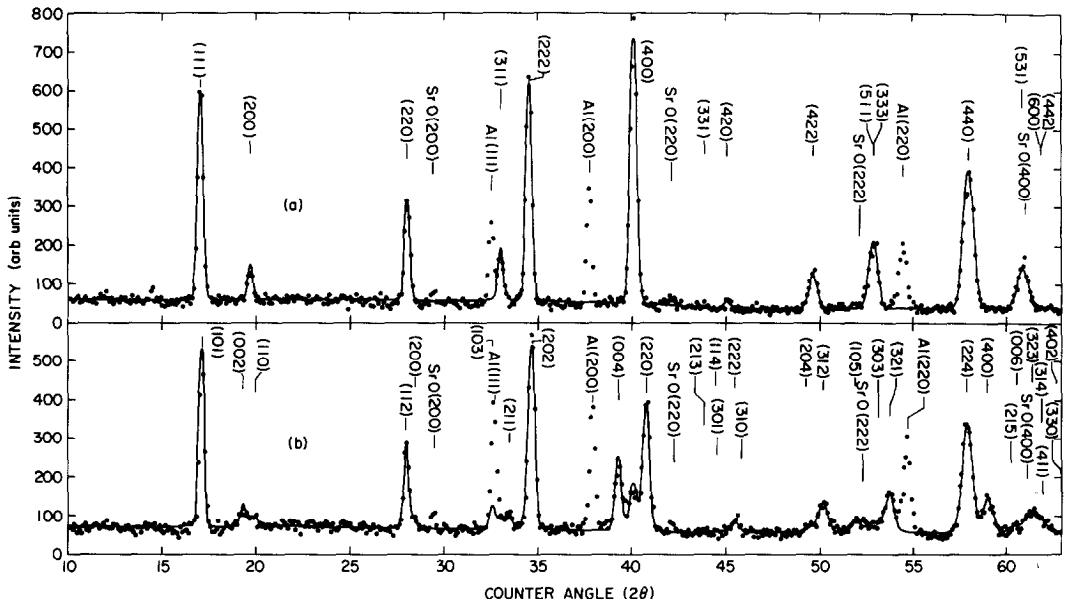

FIG. 2. Low-angle neutron diffraction patterns for Sr_2IrD_5 at (a) room temperature and (b) 4.2 K. The points correspond to measured intensities and the drawn curves are the calculated profiles including in (b) the contribution of the residual cubic phase. Aluminum lines are produced by the sample holder and cryostat, and those labeled SrO are attributed to a small impurity. Neutron wavelength is 1.3102 Å.

TABLE III

STRUCTURE AND THERMAL PARAMETERS AND CRYSTALLOGRAPHIC DATA FOR TETRAGONAL Sr_2IrD_5 AT 4.2 K

Space Group	*I4/mmm*
Cell constants (Å)	$a = b = 5.320$ (±0.001) $c = 7.796$ (±0.002)
Atomic positions	Sr: $4d(0, \frac{1}{2}, \frac{1}{4})$ Ir: $2a(0, 0, 0)$ D_a, D_b: $8h$ $(x, x, 0)$ with $x = 0.225$ (±0.001) D_c: $4e$ $(0, 0, z)$ with $z = 0.234$ (±0.004)
Occupation numbers of D sites	$n(D_a)$, $n(D_b)$: 0.96 (±0.03) $n(D_c)$: 0.70 (±0.04)
Atomic ratio (D/Sr_2 or D/Ir)	5.2 ± 0.2
Isotropic thermal parameters	
B_{Sr}	0.0 ± 0.2
B_{Ir}	0.2 ± 0.2
B_{D_a}, B_{D_b}	0.6 ± 0.2
B_{D_c}	4.9 ± 1.1
R factors	
R_1	4.94
R_2	20.37

to the first two strong neutron diffraction peaks of SrO: (200) and (220). In addition, the fact that the observed intensity of the (531) peak of Sr_2IrD_5 is significantly higher than the calculated value can be ascribed to the presence of the strong (400) reflection of SrO occurring at $2\theta = 61.04$.

A refined Ir–D distance of 1.714(5) Å was obtained from this analysis, in excellent agreement with the value of 1.70 Å obtained previously (*1*). This distance is reasonably close to 1.67 Å expected for a covalent Ir–H interaction (*7*). This suggests, in addition to a random disordered model containing six-, five-, and four-coordinated species, the possibility of discrete molecular $[IrD_5]^{4-}$ units.

The Structure of Sr_2IrD_5 at Low Temperature

The neutron diffraction diagram of Sr_2IrD_5 at 4.2 K is shown in Fig. 2b. It is quite different from that obtained at room temperature and cannot be indexed on a cubic cell. A careful study of this diagram showed that all the prominent peaks could be indexed on a tetragonal cell, but that some intensity remained at positions corresponding to the room-temperature cubic phase. This suggested that the sample at 4.2 K consisted of two phases of different structure with the major component being tetragonal and the minor constituent the untransformed cubic phase. Thus, for example, the (400) reflection of the room-temperature cubic phase, which is replaced by a clearly resolved triplet at 4.2 K, is considered to be composed of the strong (004) and (220) reflections of the tetragonal phase and the much weaker (400) peak of the residual cubic phase. The analysis based on the coexistence of two phases will be more fully

TABLE IV

OBSERVED AND CALCULATED NEUTRON DIFFRACTION DATA FOR TETRAGONAL Sr_2IrD_5 AT 4.2 K

$h\,k\,l$	2θ (°)	I_{obs}	I_{calc}	$h\,k\,l$	2θ (°)	I_{obs}	I_{calc}
1 0 1	17.12	1314	1294	4 3 1	76.81	5	4
0 0 2	19.32	208	203	5 1 0	77.76	2	1
1 1 0	20.03	70	71	3 1 6	79.12	295	304
1 1 2	27.98	632	626	4 2 4	80.33	49	63
2 0 0	28.49	65	70	2 1 7	80.98	20	19
2 0 2	34.67	1668	1641	5 1 2	81.05	448	414
0 0 4	39.25	891	858	4 1 5	82.42	169	147
2 2 0	40.74	1571	1492	5 0 3	83.38	233	224
2 1 3	43.81	38	46	4 3 3	83.38	1	1
1 1 4	44.46	0	8	5 2 1	83.86	15	15
3 0 1	44.50	0	0	0 0 8	84.46	212	204
2 2 2	45.47	189	143	1 1 8	87.94	0	1
3 1 0	45.81	0	1	3 0 7	87.96	0	1
2 0 4	49.22	24	31	4 4 0	88.28	331	284
3 1 2	50.16	456	428	4 0 6	89.61	57	50
1 0 5	51.90	221	193	3 3 6	93.09	210	230
3 0 3	53.11	0	3	3 2 7	94.92	220	208
3 2 1	53.70	632	587	5 3 2	95.00	156	147
2 2 4	57.87	1487	1465	6 0 0	95.24	29	27
4 0 0	58.99	661	656	5 0 5	96.36	216	216
2 1 5	60.28	76	89	4 3 5	96.36	6	6
0 0 6	60.53	27	37	4 2 6	96.57	309	314
3 2 3	61.37	382	388	6 1 1	97.80	40	42
3 1 4	61.89	1	1	2 2 8	98.40	605	627
4 1 1	61.92	207	197	6 0 2	98.50	105	108
4 0 2	62.70	60	67	1 0 9	100.01	78	67
3 3 0	62.96	5	8	4 4 4	101.30	531	485
4 1 3	69.04	129	131	3 1 8	101.93	12	11
4 2 2	70.28	575	553	4 1 7	101.95	88	82
4 0 4	73.19	889	876	6 2 0	102.27	473	438
1 0 7	73.85	62	55	5 2 5	103.42	8	7
3 2 5	75.34	352	370	6 1 3	104.40	40	34
2 2 6	75.56	78	83	5 3 4	104.87	61	52
3 3 4	76.78	7	6	5 4 1	104.90	352	300
5 0 1	76.81	362	273	6 2 2	105.61	29	26

justified by the final intensity calculations.

The indices of the tetragonal reflections are found to obey the restriction $h + k + l = 2n$ and hence the cell is body centered. Assuming a center of symmetry, and noting the absence of glide-plane extinctions, refinement was attempted in space group $I4/mmm$. In order to obtain an "experimental" data set for the tetragonal phase, the calculated diffraction intensities of the room-temperature cubic phase were multiplied by a factor determined by the intensity of an isolated low-temperature cubic reflection and then subtracted point by point from the observed 4.2 K diffraction pattern. Results of the profile refinement are shown in Table III and Fig. 2b; observed and calculated intensities of the Bragg peaks are presented in Table IV. Comparing intensities of the cubic and tetragonal phases it was estimated that approximately 13% of the sample at 4.2 K existed in the cubic modification. Because of this low concentration, it was not possible to verify independently that the cubic structure was unchanged in going from high to low temperature.

As a measure of the internal consistency of the refinement procedure, various statistical tests were applied to the 70 observed intensities resolved by the analysis (Table III) in order to detect the presence of a center of symmetry. The variance test (*5*) gave $V = \overline{(z - \bar{z})^2} = \overline{(I - \bar{I})^2}/\bar{I}^2 = 1.986 \approx 2$, and the result of the zero-moment test (*6*) is shown in Fig. 3. Both confirmed that the tetragonal structure has a center of symmetry. Furthermore, since the introduction of additional refinement parameters did not produce significant improvement, the most probable space group was taken to be $I4/mmm$.

Figure 4 shows the relationship of the face-centered cubic unit cell and body-centered tetragonal cell. When the temperature decreases from room temperature, the $a-b$

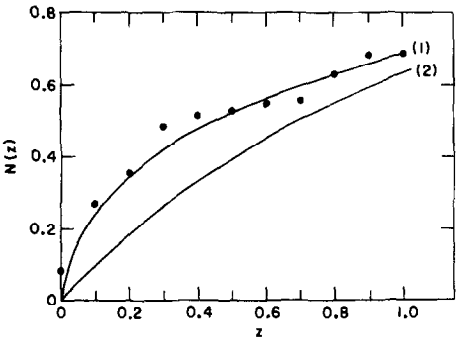

FIG. 3. Distribution functions for (1) centrosymmetric and (2) noncentrosymmetric structures [Ref. (*6*)]. Points represent experimental data for tetragonal Sr_2IrD_5.

plane contracts isotropically and c axis expands, leading to the tetragonal unit cell; at the same time, the occupation numbers of the sites D_a and D_b (see Fig. 1b) increase almost to 1, and the occupation number of the site D_c decreases to ~0.7.

The results of the refinement with the low-temperature data (Table III) can be interpreted in terms of a tetragonally distorted IrD_5 square pyramid, with the four equatorial Ir–D distances [1.693(7) Å] markedly shorter than the unique axial Ir–D distance [1.82(3) Å]. Interestingly, the weighted average of these bond lengths, (0.8)(1.693) + (0.2)(1.82) = 1.718 Å, is essentially identical to the Ir–D distance measured for the room-temperature cubic phase (1.714 Å).

A neutron pattern was also obtained at 77 K. It was much the same as that at 4.2 K, and there was no significant difference between the results of the profile refinements obtained at the two temperatures.

The Cubic–Tetragonal Transition

The phase transformation was followed by monitoring the splitting of the cubic (400) reflection into the (004) and (220) of the tetragonal structure. The temperature of the sample was decreased in stages and scans were taken at each temperature over the range in 2θ from 39.5° to 42.5°. No change in the pattern was observed until about 200 K. As evident in Fig. 5, only a slight broadening is seen at 195 K, whereas at 190 K the peak is definitely split. Figure 6 shows a series of runs at 190 K taken under conditions of improved resolution, at 2-hr intervals. On this time scale it was not pos-

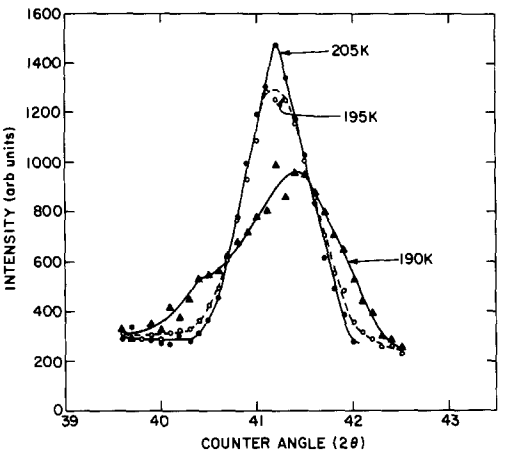

FIG. 5. Temperature dependence of intensity in the region of the cubic (400) reflection (low resolution).

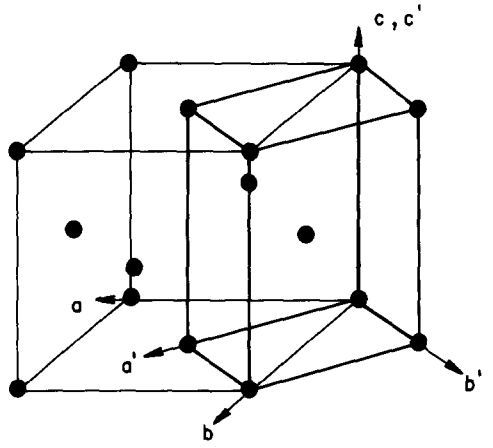

FIG. 4. Relationship between the room-temperature cubic unit cell and the low-temperature tetragonal unit cell.

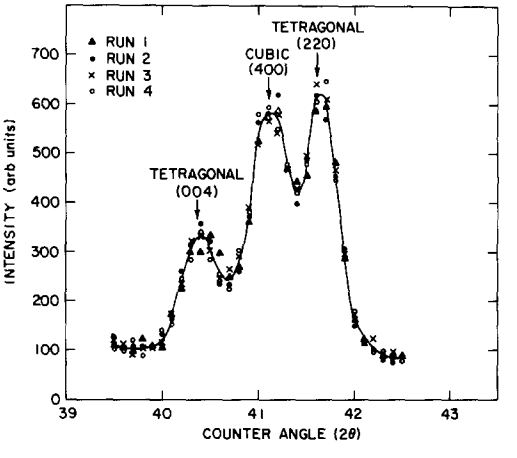

FIG. 6. Scans at 190 K, with improved resolution, showing coexistence of cubic and tetragonal phases. Successive runs were taken at 2-hr intervals and indicate rapid equilibration.

sible to detect any change in the ratio of the cubic to the tetragonal peak intensities beyond that which was established almost immediately on reaching temperature. As the temperature was decreased further, the cubic (400) continued to decrease and the tetragonal peaks to grow, with no noticeable increase in equilibration time and no change in line positions. Intensity changes ceased below about 140 K and, in fact, the pattern at that temperature was indistinguishable from that at 4.2 K, where, as we have seen, the transformation is still incomplete. On reheating, no significant hysteresis was observed. At 205 K the tetragonal peaks had disappeared and the shape of the cubic line reproduced that seen with decreasing temperature.

Discussion

Both the cubic and tetragonal structures of Sr_2IrD_5 can be considered to be made up of square pyramidal IrD_5 units (Fig. 7), sixfold disordered in the high-temperature (cubic) phase and two fold disordered in the low-temperature (tetragonal) phase. In both cases, the Ir atom is crystallographically required to be coplanar with the equatorial arrangement of four deuterium atoms. (On the other hand, the random coordination model may explain the failure of the transformation to go to completion inasmuch as hydrogen diffusion over longer distances would be required.)

Discrete binary metal hydride units involving transition metals have now been found in several compounds. The classic $[ReH_9]^{2-}$ ion [Re–H = 1.68 Å] was first discovered by single-crystal neutron diffraction in K_2ReH_9 (*8*), and we have very recently found, using single-crystal X-ray methods, the existence of octahedral $[FeH_6]^{4-}$ anions [Fe–H = 1.69(9) Å] in $FeH_6Mg_4Br_4(THF)_8$ (*9*). Furthermore, square-planar RhH_4 units [Rh–H = 1.90 Å]

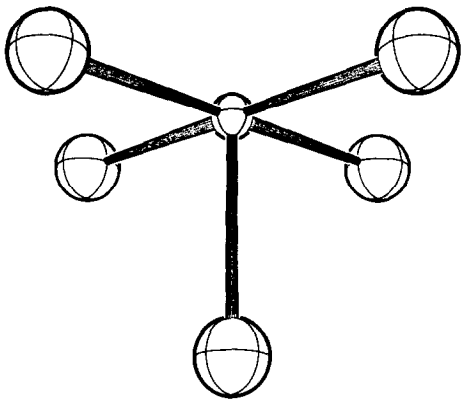

FIG. 7. A molecular plot of an isolated IrD_5 unit, based on the analysis of the cubic phase data.

have been reported by Lundberg *et al.* in Li_4RhH_4 (*10*), while Sr_2RuD_6 has been shown, through our earlier powder neutron diffraction work (*1*), to contain octahedral RuD_6 units [Ru–D = 1.69 Å]. Whether the metal hydride units in the latter two species, and in the title compound, can be considered *bona fide* anions (i.e., $[RhH_4]^{4-}$, $[RuD_6]^{4-}$ and $[IrD_5]^{4-}$) is unclear. Nevertheless, it is interesting to speculate on the existence of an entire series of stable binary metal hydride anions that might resemble the well-known $[ReH_9]^{2-}$ ion. A structural phase transformation, which appears to be similar to that observed here, has been reported (*11*) for the closely related compound Mg_2NiD_4. In this case, the ordered phase may be expected to exhibit square-planar NiD_4 units.

References

1. R. O. MOYER, JR., C. STANITSKI, J. TANAKA, M. KAY, AND R. KLEINBERG, *J. Solid State Chem.* **3**, 541 (1971).
2. H. M. RIETVELD, *J. Appl. Crystallogr.* **2**, 65 (1969).
3. A. W. HEWAT, U. K. Atomic Energy Research Group Report RLL 73/897 (1973). (Unpublished)
4. SWANSON *et al.*, NBS Circular 539, Vol. V (1955).
5. A. J. C. WILSON, *Research* **4**, 141 (1951).

6. E. R. HOWELLS, D. C. PHILLIPS, AND D. ROGERS, *Acta Crystallogr.* **3,** 210 (1950).
7. R. G. TELLER AND R. BAU, *Struct. Bonding* **44,** 1 (1981).
8. S. C. ABRAHAMS, A. P. GINSBERG, AND K. KNOX, *Inorg. Chem.* **3,** 558 (1964).
9. R. BAU, D. M. HO, AND S. G. GIBBINS, submitted for publication.
10. L. B. LUNDBERG, D. T. CROMER, AND C. B. MAGEE, *Inorg. Chem.* **11,** 400 (1972).
11. J. SCHEFER, P. FISCHER, W. HÄLG, F. STUKI, L. SCHLAPBACH, J. J. DIDISHEIM, K. YVON, AND A. F. ANDRESEN, *J. Less Common Met.* **74,** 65 (1980); J. GENOSSAR AND P. S. RUDMAN, *J. Phys. Chem. Solids* **42,** 611 (1981); D. NORÉUS AND P. E. WERNER, *Mater. Res. Bull.* **16,** 199 (1981).